To move or not to move? Functional role of ventral premotor cortex in motor monitoring during limb immobilization

Francesca Garbarini[1*], Luca Cecchetti[2], Valentina Bruno[1], Angela Mastropasqua[3], Carlotta Fossataro[1], Giuseppe Massazza[4], Katiuscia Sacco[5,6], Maria Consuelo Valentini[6,7], Emiliano Ricciardi[2], Anna Berti[1,7]

1. SAMBA – SpAtial, Motor & Bodily Awareness – Research Group, Psychology Department, University of Turin, Turin, Italy
2. MOlecular MInd Lab, IMT School for Advanced Studies Lucca, Lucca, Italy
3. German Center for Vertigo and Balance Disorders, Klinikum Grosshadern, LMU Munich, Germany
4. Physical medicine and Rehabilitation, Department of Surgical Sciences, University of Turin, Italy
5. Imaging and Plasticity Research Group, Psychology Department, University of Turin, Turin, Italy
6. Department of Neuroradiology, Azienda Ospedaliera Universitaria Città della Salute e della Scienza, Turin, Italy
7. Neuroscience Institute of Turin (NIT), Turin, Italy

***Corresponding author:** Garbarini Francesca, Department of Psychology, University of Turin, 10123 Torino, Italy. E-mail: francesca.garbarini@unito.it

Running Title: To move or not to move?

Abstract

Anatomo-clinical evidence from motor-awareness disorders after brain-damages suggests that the premotor cortex (PMC) is involved in motor-monitoring of voluntary actions. Indeed, PMC lesions prevent patients from detecting the mismatch between intended, but not executed, movements with the paralyzed limb. This fMRI study compared, in healthy subjects, free movements against blocked movements, precluded by a cast. Cast-related corticospinal excitability changes were investigated by using TMS. Immediately after the immobilization, when the cast prevented the execution of left hand movements, the contralateral right (ventral) vPMC showed both increased hemodynamic activity and increased functional connectivity with the hand area in the right somatosensory cortex, suggesting a vPMC involvement in detecting the mismatch between planned and executed movements. Crucially, after one week of immobilization, when the motor system had likely learned that no movement could be executed and, therefore, predictions about motor consequences were changed, vPMC did not show the enhanced activity as if no incongruence has to be detected. This can be interpreted as a consequence of the plastic changes induced by long-lasting immobilization, as also proved by the cast-related corticospinal excitability modulation in our subjects. The present findings highlight the crucial role of vPMC in the anatomo-functional network generating the human motor-awareness.

Keywords: brain plasticity; fMRI; long-lasting immobilization; motor control; premotor cortex.

Introduction

Actions are generated through a chain of neurobiological events that is often not available to consciousness, although we are usually aware of moving (or not moving) different parts of our body. How is this motor awareness built up in our brain? An influential model of action generation (Blakemore et al. 2002; Haggard 2005) proposed that, during voluntary movements, the central nervous system exerts a motor control on our actions by comparing motor outflow and sensory inflow. According to this model, once motor programs are selected and sent to muscles, an efference copy of the motor commands is formed and, on the basis of this signal, a forward model predicts the sensory consequences of the movement. Then, when the movement occurred, the actual sensory feedbacks are compared with the sensory predictions, to ensure that motor output matches current intentions. When the sensory feedbacks do not match the predictions, an error signal is generated to alert the system of the lack of congruency between the intended and the executed action.

An important contribution to the understanding of the anatomical counterpart of this motor monitoring system comes from the study of neuropsychological disorders in which movement awareness is dramatically impaired, as in the anosognosia for hemiplegia (AHP) (Langer and Levine 2014). In this pathological condition, brain-damaged hemiplegic patients are firmly convinced of actually executing voluntary movements with their paralyzed limb. Even if AHP has been traditionally associated to right-brain damage (Vallar and Ronchi 2006), when the assessment avoids language-related problems, this disorder emerges also in left-brain patients (Sala et al. 2009). An anatomo-clinical model of AHP, based on brain lesions and behavioral data, takes into account both the spared brain areas implementing motor intentionality [e.g. supplementary motor area – SMA (Fried et al. 2011); inferior parietal cortex (Desmurget and Sirigu 2009)] and the damaged premotor cortex (PMC), and neighbored areas, considered the neural counterpart of the comparator system, for explaining the patients' behavior (Berti et al. 2005; Vocat et al. 2010; Garbarini et al. 2012, 2013; Gandola et al. 2014; Pia et al. 2014; Piedimonte et al. 2015, 2016; Moro et al. 2016).

This lesion pattern observed in AHP patients is supposed to prevent AHP patients from detecting the mismatch between the intended (due to spared SMA), but not executed (due to damaged motor pathways), movement with the paralyzed limb. Thus, according to the classical neuropsychological inference, it has been proposed that PMC is part of a circuit that may play a crucial role in motor monitoring, being involved in the generation of motor awareness of voluntary actions (Berti et al. 2005). It is worth noting that, although sensory predictions strictly depend upon motor intention, this model implies that motor intention signals and motor comparator signals are separated and possibly generated by different motor areas. Moreover, the 'intention' considered in this model is related to the programming of the subject's voluntary action and not to the capability to understanding others' motor act, which depends on the activity of the mirror neuron system (Nelissen et al. 2011).

It is well known that other brain areas, namely the posterior parietal cortex (PPC) and the cerebellum, also play an important role in motor monitoring during voluntary actions. The PPC has been shown to be involved in detecting the mismatch between desired and actual movements, particularly when visual feedback is relevant for action execution (Desmurget et al. 1999). Consistently, during fMRI versions of prismatic adaptation task, when participants point at targets under visual guidance while wearing prism lenses that displace the visual field laterally, the activity of parieto-cerebellar circuits was primarily implicated in detecting the mismatch between visual and proprioceptive inputs (Luauté et al. 2009; Chapman et al. 2010). According to several findings (for a review see Ishikawa et al. 2016), the cerebellum plays a crucial role in acquiring and maintaining forward models for motor control, by receiving inputs from the premotor areas through the cortico-ponto-cerebellar pathway and by projecting back to the premotor areas through the cerebello-thalamo-cortical (Horne and Butler 1995). Thus, these two regions may work in parallel to predict the sensory consequences of the movement and to make movement adjustments and corrections. However, in the present study, we were focused on the motor component of the comparator system and we adopted an *a priori* hypothesis-driven approach to test the role of PMC in motor monitoring.

To this aim, we reasoned that a good way is to contrast, in normal subjects, conditions in which movement execution corresponds to the intended movement and conditions in which the intended movement is not executed. In this latter condition, the comparator system should be alerted because the sensory feedbacks would not match the intention signal. To this aim, by using functional Magnetic Resonance Imaging (fMRI), we contrasted conditions in which healthy subjects were free to move both hands (free conditions) with conditions in which left hand movements were prevented by a cast (blocked conditions). Functional responses to a hand motor task were collected just before and immediately after the left hand was immobilized (Day 1: first day of scanning) and after one week of immobilization, just before and immediately after the cast was removed (Day 2: second day of scanning, seven days later than the first scanning). See details in Methods and in Figure 1a and 1b. Note also that a Transcranial Magnetic Stimulation (TMS) experiment was designed to control that long-lasting immobilization actually induced plastic changes in the corticospinal excitability.

Although there are important differences between patients' paralysis and normal subjects' immobilization, nonetheless our experimental manipulation recreates, in healthy subjects, a condition similar to the pathological context in which hemiplegic patients plan to move, but they cannot move because of the paralysis. Indeed, during blocked conditions, when the subjects are asked to move their hands but the cast prevents the movement execution, efferent and afferent signals are likely incongruent, and a comparator system should detect the mismatch. Would the PMC activity be modulated, in this latter condition, according to its supposed comparator system function? Can the duration of the immobilization affect the activity of the comparator system in PMC? Our prediction is that different PMC activities should be expected as a consequence of the presence/absence of the cast and of the duration of the immobilization.

Material and Methods

Participants

Twenty volunteers (7 men, mean age = 22.1 years, SD= 2.1; educational level =15.8 years, SD=1.5) participated in the study. All participants were right handed, as determined by the Edinburgh Handedness Inventory (Oldfield 1971). Participants were naive to the purpose of the experiment; none of them had history or evidence of neurological and psychiatric illness and contraindication to Transcranial Magnetic Stimulation (TMS) (Rossi et al. 2009; Bruno, Fossataro, and Garbarini 2017). All participants gave informed written consent. The investigation was approved by the Ethics Committee of the University of Turin (protocol A290114) and conforms to the Declaration of Helsinki.

Experimental procedure

The first day (i.e., Day 1), participants performed inside the scanner a hand motor task (open/close right or left hand alternately) in free condition (T1); at the end of the scanning session, participants' left hand was immobilized with a cast and they performed the same task with the left hand blocked and the right hand free (T2). The second day (i.e., Day 2), after one week of immobilization, the task was performed as in T2, with the left hand blocked and the right hand free (T3); at the end of the scan, the cast was removed from the left hand and the task was performed with both hand free (T4) (Figure 1a).

One week before T1 and immediately after T4, participants underwent two sessions of TMS in order to investigate plasticity effects on corticospinal system induced by the immobilization.

In a control experiment, acquired in a separated session, the participants were asked to perform a motor imagery task, consisting in the same paradigm used in the motor task (including the same set of stimuli) with the only difference that the subjects had to imagine the hand movement (with a kinesthetic motor imagery, (Jeannerod 1995; Piedimonte et al. 2014; Bisio et al. 2017; Bruno et al. 2018) instead of moving the hand (as in free conditions) or trying to move the hand (as in blocked conditions).

Immobilization procedure

We replicated the same immobilization method used by Burin and colleagues (Burin et al. 2017). The rationale behind immobilizing the hand and arm was that the hand/finger movements had to be completely prevented. Thus, immobilization of the wrist, metacarpophalangeal (MCP) joints, proximal interphalangeal (PIP) and distal interphalangeal (DIP) joints was obtained with a palmar thermoplastic splinting. The wrist joint was in 30-45 degrees of extension, the MCP joints in 60 to 70 degrees of flexion, the PIP and DIP joints were extended and the thumb was abducted.

fMRI paradigm

Participants were asked to move (or try to move, in blocked conditions) their right hand and left hand alternately. In rest condition, they had to relax, without performing any movements. The movement consisted in the flexion and extension of the five fingers conjointly. A special pillow was placed under each hand, and the wrists were tied down. Subjects moved their hand after the presentation of a visual stimulus always representing the two hands. When both hands were white, the subjects had to stay still (rest condition). When the right/left hand gradually became red, participants had to prepare the corresponding hand movement (preparation phase). When the right/left hand turned completely red participants had to move the corresponding hand, i.e. to open/close the hand (movement execution phase). The experimental design included 12 trials in which participants had to move the right hand and 12 trials in which they had to move (or try to move) the left hand. Hand movements were self-paced. The task was performed using a block design with 12 s of rest, 6 s of motor preparation and 12 s of motor execution condition. The whole task lasted about 12 minutes (Figure 1b). During the imagery task, the very same paradigm was used with the only difference that participants had to imagine the hand movement. Stimuli presentation was handled by using the E-prime 2.0 software (Psychology Software Tools, Inc., Pittsburgh, PA, https://www.pstnet.com/eprime.cfm) via the RM compatible visual stimulation device (VisuaStim-Resonance Technologies, Northridge, USA).

fMRI data acquisition

Data were acquired using a 3 Tesla 32-Channel Digital Head Coil scanner Intera (Philips, 32-Channel Digital Head Coil). Functional T2*-weighted images were acquired using echo planar imaging (GRE-EPI; TR = 1.500ms; TE = 35ms; FA = 90°; FOV = 230x230mm; acquisition matrix = 68x64; reconstruction matrix = 80x80; slice thickness = 3mm (10% gap); acquisition voxel size = 3.382x3.594x3.3mm; reconstruction voxel size = 2.875x2.875x3.3mm; 24 ascending axial oblique slices; 488 volumes; 1 run; ~12min of acquisition time). Since our main interest was to record activity of the motor system, rather than of the whole brain, we adopted a partial brain coverage scheme, where axial slices were prescribed running parallel to the sylvian fissure, covering from the top of the brain to the opercular territories. This helped also in maintaining the repetition time sufficiently short, which is an important feature for connectivity analysis. In the same session, a 3D high-resolution T1w image was acquired for each participant (FFE, TR = 8.207ms; TE = 3.759ms; FA = 8°; FOV = 256x256mm; acquisition matrix = 256x256; slice thickness = 1mm; voxel size = 1x1x1mm; 180 sagittal slices).

fMRI data analysis

fMRI data analyses were performed using SPM12 (Ashburner 2012) and AFNI (Cox 1996). For each timepoint (i.e., T1, T2, T3 and T4) and each subject we measured brain activity during the movement execution and the preparatory phase of the motor task. In brief, raw functional images were standardly preprocessed in SPM12 (i.e., slice timing correction, motion correction, T1w coregistration, 6mm FWHM Gaussian spatial smoothing, intensity normalization) and the obtained volumes were included in a general linear model (GLM) as the dependent variable. Four regressors of interest (i.e., right hand movement, left hand movement, right hand preparatory phase, left hand preparatory phase) were convolved with the canonical hemodynamic response function and were added to the GLM as explanatory variables. In addition, the six head motion parameters (rotations

and translations on the x, y and z axes), derived from the motion correction preprocessing step, were included in the model as nuisance variables. This single-subject analysis pipeline produced four ß-values maps, each representing blood oxygenation level dependent (BOLD) signal for a specific regressor of interest (e.g., right hand movement). Afterwards, aiming to aggregate single-subject results into a group-level analysis, T1w images were spatially transformed to match the MNI/ICBM template (2x2x2mm spatial resolution) using a non-linear algorithm (Ashburner and Friston 1999) and the computed deformation field was then applied to ß-values maps.

Since our interest was to test an *a priori* hypothesis, rather than running a whole-brain analysis, we used NeuroSynth (Yarkoni et al. 2011) (http://neurosynth.org) and reverse inference maps to identify term-based meta-analytic coordinates for brain regions commonly implicated in hand movements. Therefore, a region of interest (ROI) for the primary motor cortex (M1) devoted to hand movements control was obtained by drawing a sphere (6mm radius) centered at the peak value for the reverse inference map of the term *"hand"* (left hemisphere; x=-36, y=-22 z=+56; 736 studies). The correctedness of this procedure was testified also by the spatial overlap between the location of the peak for this meta-analytic map and the well-known "omega" landmark for the hand motor cortex. Thus, an identical approach was used to define the left SMA (term: *"supplementary motor"*; x=-4, y=-6, z=+58; 607 studies), the left dPMC (term: *"dorsal premotor"*; x=-26, y=-10, z=+62; 165 studies) and the left vPMC (term: *"ventral premotor"*; x=-56, y=+6, z=+30; 161 studies). Specular coordinates (i.e., positive x values, while keeping y and z constant) were used to define four right hemisphere ROIs (right M1, right SMA, right dPMC and right vPMC). For each subject (n=20), timepoint (n=4) and ROIs (n=8), we extracted ß-values related to both the preparatory phase and the motor execution phase for the contralateral hand movement (e.g, left M1 activity while moving the right hand). These values were entered, as dependent variables, in two separate 2x2x2 MANOVA, one for the preparatory phase and the other for the actual motor execution phase. Three two-levels within-subject factors, “Side” (Left hand; Right hand), “Time” (Day 1; Day 2) and “Cast” (Free; Blocked) and a full factorial design were used to investigate brain

activity following motor immobilization, at group-level. Post-hoc comparisons were computed and corrected for multiple comparisons using Bonferroni. The MANOVA and post-hoc analyses were carried out using SPSS statistical software (IBM, Chicago, IL). To rule out the possibility that the modultory effect of cast on the selected ROI could reflect mental simulation during motor imagery, we performed paired t-test (two tailed), comparing ß-values of the motor imagery task with ß-values of the motor task at T1, T2, T3, T4. This allowed to discriminate between the blocked conditions of the motor task (T2 and T3), in which the subjects were asked to "try" to move their blocked hand, and a motor imagery task, in which the hand movement has to be mentally simulated.

Furthermore, to estimate the context-dependent functional connectivity between right vPMC and the rest of the brain during the motor execution phase, we used the Generalized Psycho-Physiological Interaction (gPPI) (McLaren et al. 2012) analysis as implemented in AFNI (Cox 1996). Here, we selected the AFNI pipeline for two methodological reasons: first, in our experiment the motor execution phase has a relatively short duration and, as a consequence, the use of deconvolution is crucial (Gitelman et al. 2003); importantly, the deconvolution process in AFNI is invertible and robust to the mean centering effect (Di et al. 2017). Second, in AFNI psychological effects are removed from the physiological variable before calculating gPPI, hence reducing the collinearity between the interaction terms and the main effect regressors (Di et al. 2017). Moreover, since correlation analysis is more subject to spurious results induced by motion artifacts (Power et al. 2012), functional data were preprocessed with an optimized pipeline. Other than the standard preprocessing steps (i.e., slice timing correction, motion correction, T1w coregistration, 6mm FWHM Gaussian spatial smoothing, intensity normalization) we estimated motion outliers using the framewise displacement metric as proposed by Power and colleagues (Power et al. 2012) and the resulting regressors were included in the gPPI analysis as nuisance variables (i.e., spike regression method, Satterthwaite et al., 2013). The four regressors of interest (i.e., right hand movement, left hand movement, right hand preparatory phase, left hand preparatory phase) were included in the gPPI analysis as main effects (i.e., psychological components), while the

physiological component was represented by the preprocessed timeseries extracted from the right vPMC (6mm spherical ROI). The PPI term was then obtained as the interaction between the right vPMC activity and the regressor for left hand movements. Single-subject gPPI maps were then spatially transformed to match the MNI space (2x2x2mm voxel resolution), using a non linear registration algorithm (3dQwarp) and constituted the dependent variable in a 2x2 ANOVA full-factorial design with "Time" and "Cast" as main factors. The significance of gPPI analysis was assessed at group-level by means of a permutation test (FSL randomise, Winkler, Ridgway, Webster, Smith, & Nichols, 2014) and the threshold free cluster-enhanced method (Smith and Nichols 2009). Additionally, to confirm the ROI-based results, whole-brain analysis is presented in Supplementary Material.

TMS procedure and analysis

Participants underwent two sessions of TMS in order to investigate cortical modifications induced by the immobilization. TMS pulses were administered using a Magstim Rapid^2 stimulator (Magstim, Whitlan, Dyfed, Wales, UK) connected to a 70-mm figure-of-eight coil positioned over the left and right M1. The resting motor threshold (rMT) was defined as the lowest stimulus intensity capable of evoking 5 out of 10 motor evoked potentials (MEPs) with at least 50 μV peak-to-peak amplitude (Rossini et al. 2015). The rMT and MEPs were recorded before and after immobilization. In the pre-immobilization session, rMT and MEPs were recorded one week before T1, in order to avoid any possible effect of TMS on the fMRI results. For the same reason, we did not acquire TMS before T2, T3 and T4. In the post-immobilization session, rMT and MEPs were recorded immediately after T4 (thus the same day of the second scanning). During MEPs recording session (10 MEPs were collected for the right and 10 MEPs for the left hand), the stimulator intensity was set at 120% of the individual rMT. MEPs were recorded from the first dorsal interosseous (FDI) muscle of participants' right and left hands. Electromyographic (EMG) activity was recorded by pairs of Ag–AgCl surface pre-gelled electrodes (35 mm diameter) connected to a

Biopac MP-150 electromyograph (Biopac Systems Inc., Santa Barbara, CA). The EMG signal was acquired according to the method used in previous studies (Bucchioni et al. 2016; della Gatta et al. 2016; Bruno, Fossataro, Bolognini, et al. 2017; Fossataro et al. 2018). MEPs were analyzed off-line. In the data analysis, with respect to rMT, according to the non-normality of the residuals distribution (Shapiro-Wilk test), non-parametric Wilcoxon matched-pairs tests were performed to compare the rMT pre- and post-immobilization of the right and left hemisphere. With respect to MEPs amplitude, according to the normality of the residuals distribution (Shapiro-Wilk test), a 2x2 repeated measures ANOVA was performed, with Hand (Left; Right) and Time (Pre; Post immobilization) as within-subjects factors.

Results

fMRI results

According to the meta-analytic approach (Yarkoni et al. 2011) described in methods, ROIs analysis on the brain areas commonly implicated in the hand movements (M1, SMA, vPMC and dPMC) revealed the following results. See maps comparing both motor preparation and motor execution with rest activity in Supplementary Figure 1 and 2.

In the preparation phase, the MANOVA model on the ß-values extracted from the eight ROIs did not show any significant results. For the movement execution phase, the MANOVA revealed a significant overall effect for Side*Cast ($F_{(4,16)}$=13.240, p<0.001, η_p^2=0.768) and Side*Day*Cast ($F_{(4,16)}$=3.667, p=0.026, η_p^2=0.478) interactions. Notably, these results were driven by changes in contra-immobilization M1 and vPMC activity, whilst SMA and dPMC showed no significant modulations.

M1 activity: *Side*Cast interaction* ($F_{(1,19)}$=7.963, p=0.01, η_p^2=0.295). A significant difference between blocked and free conditions was found only for the left (manipulated) hand. Post hoc comparisons showed that, when the left hand was immobilized by the cast, the contralateral right M1 activity was significantly lower with respect to free conditions (p=0.013). See Figure 1c.

vPMC activity: *Side*Cast interaction* ($F_{(1,19)}$=31.514, p<0.001, η_p^2=0.624). A significant difference between blocked and free conditions was found only for the left (manipulated) hand. However, contrary to the M1 activity, when the left hand was immobilized by the cast, the activity of the contralateral right vPMC was significantly higher with respect to free conditions (p=0.040). Coherently, a significant difference between left and right vPMC was found only in blocked condition (p=0.001), while in free conditions left and right vPMC were similarly activated. See Figure 1d.

*Side*Time*Cast interaction* ($F_{(1,19)}$=13.852, p<0.001, η_p^2=0.422). For the left (manipulated) hand, a significant difference between blocked and free conditions was found only in Day 1. Post hoc comparisons showed that the activity of the contralateral right vPMC significantly increased at T2 (as soon as the left hand was immobilized) compared to T1 (p=0.023). See Figure 1e.

For both M1 and vPMC, no significant results were found for the right control hand.

In the control motor imagery task, we found that the activity of the right vPMC was significantly lower with respect to all the four timepoints of the motor task, including free (T1 and T4) and blocked (T2 and T3) conditions. See Supplementary Figure 3. See the results of the additional whole-brain analysis in Supplementary Material and in Supplementary Figure 4.

Furthermore, the gPPI, used to estimate the context-dependent functional connectivity between right vPMC and the rest of the brain, revealed a main effect of Cast (p<0.05 TFCE corrected). This suggests that, when the left hand was immobilized, the contralateral right vPMC activity was significantly more coupled with activity in right primary somatosensory cortex (S1; x=+55, y=-17, z=+43; See Figure 1f). Of note, according to the Neurosynth database (11406 studies, January 2018), this region demonstrates high posterior probability scores - P(Term|Activation) - for terms such as "somatosensory cortices" (P = 0.91; Z-scores = 9.32), "tactile" (P = 0.86; Z-scores = 8.09), "touch" (P = 0.85; Z-scores = 5.15), "index finger" (P = 0.84; Z-scores = 4.12) and "finger" (P = 0.80; Z-scores = 5.87). This evidence confirms the anatomical specificity of our functional connectivity results.

TMS results

Wilcoxon matched-pairs tests on rMT found a significant increase of rMT of the right hemisphere (contralateral to the manipulated hand) in post- with respect to pre-immobilization ($T=6$, $p<0.001$) (right hemisphere rMT: mean ± sd; Pre: 54.95±7.32; Post: 60±8.45). No significant difference was found for left hemisphere in post- with respect to pre-immobilization ($T=104.5$; $p=0.99$) (left hemisphere rMT: mean ± sd; Pre: 53.85±7.50; Post: 54.6±7.63). A significant difference was found between left and right hemisphere only in post-immobilization ($T=29.5$; $p=0.01$). See Supplementary Figure 5. ANOVA on MEPs amplitude did not find any significant main effects, confirming that, for the left hemisphere, different rMT between pre- and post-immobilization produced comparable MEPs.

Discussion

In the present study we used limb immobilization in order to study whether motor areas proposed to be involved in motor programming and monitoring were modulated by the congruency between movement intention and movement execution.

Our results first provide compelling evidence for a functional role of PMC in motor monitoring of voluntary action. Indeed, according to our predictions, the activity of PMC (and particularly of vPMC) was modulated by the presence/absence of the immobilization and by its duration. In blocked conditions, when the sensory predictions did not match with the sensory feedbacks because no movement was actually performed with the left hand, a greater activity of the contra-immobilization right vPMC, with respect to normal movement condition, was found. This suggests an on-line vPMC involvement in detecting the mismatch between movement planning and (no) movement execution. Importantly, these vPMC results, obtained with our *a priori* hypothesis-driven ROI approach, are confirmed by whole-brain analysis (see Supplementary materials). Although the present study was focused on the motor component of the comparator system, it is

interesting to note that whole-brain analysis also revealed an involvement of the supramarginal gyrus (see Sup. Figure 4) that, as previously described (e.g. Jenmalm et al. 2006), might be involved in signaling the discrepancy between predicted and actual sensory consequences of the actions.

Interestingly, the greater activity of the right vPMC was present as soon as the left hand was immobilized (T2). After one week of immobilization, vPMC did not show any enhanced activity, as if no incongruence has to be detected. This suggests that, when the system had likely learned that no movement could be execute with the left (immobilized) hand, predictions about motor consequences are changed (i.e. the absence of movement becomes the expected output and the comparator system does not produce alerting signals). This might be a consequence of some plastic changes induced by the immobilization, as also proved by the cast-related corticospinal excitability modulation in our subjects (Facchini et al. 2002; Avanzino et al. 2011; Kaneko et al. 2014; Burin et al. 2017). Indeed, the motor threshold for the immobilized limb was found to be higher after one week immobilization.

It is important to note that the comparison between the motor task and the control motor imagery task showed, in all the analyzed clusters (including the crucial vPMC), a significantly reduced brain activity during motor imagery with respect to both free conditions (T1 and T4) and blocked conditions (T2 and T3) of the motor task. We acknowledge, as an important limitation of this control experiment, that data of the motor imagery task and of the motor task were collected in different experimental sessions. However, we think that this control (required by an anonymous reviewer) might suggest that the difference between real and simulated movements, extensively described in previous studies (Porro et al. 1996; Roth et al. 1996; Lotze et al. 1999; Dechent et al. 2004; Kasess et al. 2008; Garbarini et al. 2014), also pertains to the blocked conditions; i.e. it is possible to functionally discriminate between conditions in which the subjects were asked to "try" to move their blocked hand and a motor imagery task in which the hand movement has to be mentally simulated. These results can rule out the possibility that the increased activity in vPMC, observed here soon after the application of the cast (at T2), reflects a mental simulation. We also

acknowledge that, in this control experiment, we only tested the possible confounding effect of motor imagery *per se,* while the effect of immobilization on motor imagery (e.g. Bassolino et al. 2014; Burianova et al. 2016) as well as on other cognitive aspects (e.g. peripersonal space and body representation; Bassolino et al. 2015), remains outside the purpose of the present study.

Interestingly, in the contra-immobilization right hemisphere, M1 showed an opposite modulation during the task as compared to vPMC. According to previous data (Huber et al. 2006; Avanzino et al. 2011; Langer et al. 2012), M1 activity, related to the kinesthetic component of the movement, is reduced in blocked with respect to free conditions. Even if in M1 the three-way interaction is not significant, there is a trend in right M1 activity showing a progressive time-dependent reduction of BOLD signal in blocked conditions (see Supplementary Figure 6). It is worth noting that previous studies on both immobilization procedure in healthy subjects (Avanzino et al. 2011) and constraint-induced movement therapy (CIMT) in brain-damaged patients (Wittenberg and Schaechter 2009) showed increased activity of the hemisphere ipsilateral to the immobilized limb due to hyper-use of the other side, however we did not find any significant modulation in the ipsilateral (i.e., left) M1, both in TMS parameters (Supplementary Figure 5) and in BOLD signal (Supplementary Figures 6). Contrary to the cast-related decrease of the contra-immobilization M1 activity, the increase of the vPMC activity is coherent with its involvement in motor monitoring function. This is in accordance with a considerable amount of evidence suggesting that, in humans and monkeys, vPMC also sub-serves motor cognitive functions, including action and intention understanding (Nelissen et al. 2011), imitation (Rizzolatti et al. 2002; Iacoboni 2009) and even space computation (Fogassi et al. 1992, 1996; Avenanti et al. 2012). Specifically related to monitoring function, although in a different domain with respect to our study, it has been shown that, during speech production, the comparison between normal speech and perturbed speech (generating compensatory motor commands) induce increased activity in bilateral vPMC (Golfinopoulos et al. 2011).

An alternative explanation of our results would be that the increased vPMC activity in blocked conditions could be ascribed to difficulties in motor planning during left hand block at T2, as soon

as the hand was immobilized by the cast. However, the absence of cast-related modulatory effect on a classical motor planning-related area, such as SMA (Tanji and Shima 1994; Nachev et al. 2008; Garbarini et al. 2014), as well as on each hand-motor area considered in the preparation phase, does not support this hypothesis. No modulation was found also on dPMC, suggesting that, in our task, this area is functionally disentangled from vPMC (Fogassi et al. 2001; Rizzolatti and Luppino 2001; Majdandzc et al. 2009).

Ventral PMC has been also described as exerting an important role in multisensory integration processes, where motor output and sensory inputs coming from different modalities are realigned in a unique reference frame (Graziano 1999; Ehrsson et al. 2004; Makin et al. 2008; Ronga et al. 2012). Crucially, when, in our experiment, the left hand was immobilized, the right vPMC showed an increased functional connectivity with the hand area in the right S1. This may reflect an intensified flow of incongruent sensory feedbacks for the comparison with the sensory prediction based on motor planning. Similar vPMC-S1 connectivity was found in a previous study, where the ischemic nerve block was used to investigate the S1 activity when voluntary movements were performed in absence of somatosensory feedbacks (Christensen et al. 2007). Although designed with a very different rationale, that study also showed a significantly greater vPMC activity as soon as the somatosensory block occurred (Christensen et al. 2007). This represents a complementary results with respect to our study, where the movement execution was prevented but the somatosensory components were spared (see also Garbarini, Rabuffetti, Piedimonte, Solito, & Berti, 2015).

The role of contra-immobilization vPMC as a comparator system indicates that, at least in the motor context, the monitoring function is implemented in the same neural network responsible for the process that has to be controlled (Berti et al. 2005). Thus, motor functions and motor monitoring functions can be combined in two anatomo-functional models for free and blocked movements (see Figure 2). In free conditions, the congruence between intended and executed movement requires a minimal activity of the comparator system ("I moved my hand as I planned"). On the contrary, in

blocked conditions, the enhanced vPMC activity and the increased functional connectivity with S1, alert the system about the incongruence between motor intention and motor execution ("I did not move my hand as I planned").

Taken together these findings, by investigating hemodynamic activity and functional connectivity in healthy subjects during limb immobilization, provide convincing evidence of the involvement of vPMC in motor monitoring. Although motor awareness has not been directly evaluated in our sample, we may speculate that vPMC, for its crucial role in detecting the status of the motor system, is an important component for the emergence of action-related consciousness.

Acknowledgments

The authors are grateful to the volunteers involved in the study. This work has been funded by MIUR-SIR 2014 grant (RBSI146V1D) and by the San Paolo Foundation 2016 grant (CSTO165140) to F.G.

References:

Ashburner J. 2012. SPM: A history. Neuroimage.

Ashburner J, Friston KJ. 1999. Nonlinear spatial normalization using basis functions. Hum Brain Mapp. 7:254–266.

Avanzino L, Bassolino M, Pozzo T, Bove M. 2011. Use-Dependent Hemispheric Balance. J Neurosci. 31:3423–3428.

Avenanti A, Annela L, Serino A. 2012. Suppression of premotor cortex disrupts motor coding of peripersonal space. Neuroimage. 63:281–288.

Bassolino M, Campanella M, Bove M, Pozzo T, Fadiga L. 2014. Training the motor cortex by observing the actions of others during immobilization. Cereb Cortex. 24:3268–3276.

Bassolino M, Finisguerra A, Canzoneri E, Serino A, Pozzo T. 2015. Dissociating effect of upper limb non-use and overuse on space and body representations. Neuropsychologia. 70:385–392.

Berti A, Bottini G, Gandola M, Pia L, Smania N, Stracciari A, Castiglioni I, Vallar G, Paulesu E. 2005. Shared cortical anatomy for motor awareness and motor control. Science. 309:488–491.

Bisio A, Garbarini F, Biggio M, Fossataro C, Ruggeri P, Bove M. 2017. Dynamic Shaping of the Defensive Peripersonal Space through Predictive Motor Mechanisms: When the "Near" Becomes "Far." J Neurosci. 37:2415–2424.

Blakemore S-J, Frith CD, Wolpert DM. 2001. The cerebellum is involved in predicting the sensory consequences of action. Neuroreport. 12:1879–1884.

Blakemore S-J, Wolpert DM, Frith CD. 2002. Abnormalities in the awareness of action. Trends Cogn Sci. 6:237–242.

Bruno V, Fossataro C, Bolognini N, Zigiotto L, Vallar G, Berti A, Garbarini F. 2017. The role of premotor and parietal cortex during monitoring of involuntary movement: a combined TMS and tDCS study. Cortex. 96:83–94.

Bruno V, Fossataro C, Garbarini F. 2017. Report of seizure induced by 10 Hz rTMS over M1. Brain Stimul.

Bruno V, Fossataro C, Garbarini F. 2018. Inhibition or facilitation? Modulation of corticospinal excitability during motor imagery. Neuropsychologia. 111:360–368.

Bucchioni G, Fossataro C, Cavallo A, Mouras H, Neppi-Modona M, Garbarini F. 2016. Empathy or ownership? Evidence from corticospinal excitability during pain observation. J Cogn Neurosci. 28:1760–1771.

Burianova H, Sowman PF, Marstaller L, Rich AN, Williams MA, Savage G, Al-Janabi S, De Lissa P, Johnson BW. 2016. Adaptive Motor Imagery: A Multimodal Study of Immobilization-Induced Brain Plasticity. Cereb Cortex. 26:1072–1080.

Burin D, Garbarini F, Bruno V, Fossataro C, Destefanis C, Berti A, Pia L. 2017. Movements and body ownership: Evidence from the rubber hand illusion after mechanical limb immobilization. Neuropsychologia. 107:41–47.

Chapman HL, Eramudugolla R, Gavrilescu M, Strudwick MW, Loftus A, Cunnington R, Mattingley JB. 2010. Neural mechanisms underlying spatial realignment during adaptation to optical wedge prisms. Neuropsychologia. 48:2595–2601.

Christensen MS, Lundbye-Jensen J, Geertsen SS, Petersen TH, Paulson OB, Nielsen JB. 2007. Premotor cortex modulates somatosensory cortex during voluntary movements without proprioceptive feedback. Nat Neurosci. 10:417–419.

Cox RW. 1996. AFNI: Software for Analysis and Visualization of Functional Magnetic Resonance Neuroimages. Comput Biomed Res. 29:162–173.

Dechent P, Merboldt K-D, Frahm J. 2004. Is the human primary motor cortex involved in motor imagery? Cogn Brain Res. 19:138–144.

della Gatta F, Garbarini F, Puglisi G, Leonetti A, Berti A, Borroni P. 2016. Decreased motor cortex excitability mirrors own hand disembodiment during the rubber hand illusion. Elife. 5:1744–1750.

Desmurget M, Epstein CM, Turner RS, Prablanc C, Alexander GE, Grafton ST. 1999. Role of the posterior parietal cortex in updating reaching movements to a visual target. Nat Neurosci.

2:563–567.

Desmurget M, Sirigu A. 2009. A parietal-premotor network for movement intention and motor awareness. Trends Cogn Sci. 13:411–419.

Di X, Reynolds RC, Biswal BB. 2017. Imperfect (De) Convolution May Introduce Spurious Psychophysiological Interactions and How to Avoid It. Hum Brain Mapp. 38:1723–1740.

Ehrsson HH, Spence C, Passingham RE. 2004. That's my hand! Activity in premotor cortex reflects feeling of ownership of a limb. Science. 305:875–877.

Facchini S, Romani M, Tinazzi M, Aglioti SM. 2002. Time-related changes of excitability of the human motor system contingent upon immobilisation of the ring and little fingers. Clin Neurophysiol. 113:367–375.

Fogassi L, Gallese V, Buccino G, Craighero L, Fadiga L, Rizzolatti G. 2001. Cortical mechanism for the visual guidance of hand grasping movements in the monkey: A reversible inactivation study. Brain. 124:571–586.

Fogassi L, Gallese V, di Pellegrino G, Fadiga L, Gentilucci M, Luppino G, Matelli M, Pedotti A, Rizzolatti G. 1992. Space coding by premotor cortex. Exp Brain Res. 89:686–690.

Fogassi L, Gallese V, Fadiga L, Luppino G, Matelli M, Rizzolatti G. 1996. Coding of peripersonal space in inferior premotor cortex (area F4). J Neurophysiol. 76:141–157.

Fossataro C, Bucchioni G, D'Agata F, Bruno V, Morese R, Krystkowiak P, Garbarini F. 2018. Anxiety-dependent modulation of motor responses to pain expectancy. Soc Cogn Affect Neurosci.

Fried I, Mukamel R, Kreiman G. 2011. Internally generated preactivation of single neurons in human medial frontal cortex predicts volition. Neuron. 69:548–562.

Gandola M, Bottini G, Zapparoli L, Invernizzi P, Verardi M, Sterzi R, Santilli I, Sberna M, Paulesu E. 2014. The physiology of motor delusions in anosognosia for hemiplegia: implications for current models of motor awareness. Conscious Cogn. 24:98–112.

Garbarini F, D'Agata F, Piedimonte A, Sacco K, Rabuffetti M, Tam F, Cauda F, Pia L, Geminiani

G, Duca S, Graham SJ, Berti A. 2014. Drawing lines while imagining circles: Neural basis of the bimanual coupling effect during motor execution and motor imagery. Neuroimage. 88:100–112.

Garbarini F, Piedimonte A, Dotta M, Pia L, Berti A. 2013. Dissociations and similarities in motor intention and motor awareness: The case of anosognosia for hemiplegia and motor neglect. J Neurol Neurosurg Psychiatry. 84:416–419.

Garbarini F, Rabuffetti M, Piedimonte A, Pia L, Ferrarin M, Frassinetti F, Gindri P, Cantagallo A, Driver J, Berti A. 2012. "Moving" a paralysed hand: Bimanual coupling effect in patients with anosognosia for hemiplegia. Brain. 135:1486–1497.

Garbarini F, Rabuffetti M, Piedimonte A, Solito G, Berti A. 2015. Bimanual coupling effects during arm immobilization and passive movements. J Neurosci. 34:7375–7382.

Gitelman DR, Penny WD, Ashburner J, Friston KJ. 2003. Modeling regional and psychophysiologic interactions in fMRI: The importance of hemodynamic deconvolution. Neuroimage.

Golfinopoulos E, Tourville JA, Bohland JW, Ghosh SS, Nieto-Castanon A, Guenther FH. 2011. FMRI investigation of unexpected somatosensory feedback perturbation during speech. Neuroimage. 55:1324–1338.

Graziano MS. 1999. Where is my arm? The relative role of vision and proprioception in the neuronal representation of limb position. Proc Natl Acad Sci U S A. 96:10418–10421.

Haggard P. 2005. Conscious intention and motor cognition. Trends Cogn Sci. 9:290–295.

Horne MK, Butler EG. 1995. The role of the cerebello-thalamo-cortical pathway in skilled movement. Prog Neurobiol. 46:199–213.

Huber R, Ghilardi MF, Massimini M, Ferrarelli F, Riedner BA, Peterson MJ, Tononi G. 2006. Arm immobilization causes cortical plastic changes and locally decreases sleep slow wave activity. Nat Neurosci. 9:1169–1176.

Iacoboni M. 2009. Imitation, Empathy, and Mirror Neurons. Annu Rev Psychol. 60:653–670.

Ishikawa T, Tomatsu S, Izawa J, Kakei S. 2016. The cerebro-cerebellum: Could it be loci of forward models? Neurosci Res.

Ito M. 1972. Neural design of the cerebellar motor control system. Brain Res. 40:81–84.

Ito M. 2008. Control of mental activities by internal models in the cerebellum. Nat Rev Neurosci. 9:304–313.

Jeannerod M. 1995. Mental imagery in the motor context. Neuropsychologia. 33:1419–1432.

Jenmalm P, Schmitz C, Forssberg H, Ehrsson HH. 2006. Lighter or Heavier Than Predicted: Neural Correlates of Corrective Mechanisms during Erroneously Programmed Lifts. J Neurosci. 26:9015–9021.

Kaneko F, Murakami T, Kiyoshi O, Kurumadani H, Kawaguchi K. 2014. Decreased cortical excitability during motor imagery after disuse of an upper limb in humans. J Neurosci. 34:7375–7382.

Kasess CH, Windischberger C, Cunnington R, Lanzenberger R, Pezawas L, Moser E. 2008. The suppressive influence of SMA on M1 in motor imagery revealed by fMRI and dynamic causal modeling. Neuroimage. 40:828–837.

Langer KG, Levine DN. 2014. Babinski, J. (1914). Contribution to the Study of the Mental Disorders in Hemiplegia of Organic Cerebral Origin (Anosognosia). Translated by K.G. Langer & D.N. Levine. Cortex. 61:5–8.

Langer N, Hänggi J, Müller NA, Simmen HP, Jäncke L. 2012. Effects of limb immobilization on brain plasticity. Neurology. 78:182–188.

Lotze M, Montoya P, Erb M, Hülsmann E, Flor H, Klose U, Birbaumer N, Grodd W. 1999. Activation of Cortical and Cerebellar Motor Areas during Executed and Imagined Hand Movements: An fMRI Study. J Cogn Neurosci. 11:491–501.

Luauté J, Schwartz S, Rossetti Y, Spiridon M, Rode G, Boisson D, Vuilleumier P. 2009. Dynamic changes in brain activity during prism adaptation. J Neurosci. 29:169–178.

Majdandzc J, Bekkering H, Van Schie HT, Toni I. 2009. Movement-Specific Repetition

Suppression in Ventral and Dorsal Premotor Cortex during Action Observation. Cereb Cortex Novemb. 19:2736–2745.

Makin TR, Holmes NP, Ehrsson HH. 2008. On the other hand: Dummy hands and peripersonal space. Behav Brain Res. 191:1–10.

McLaren DG, Ries ML, Xu G, Johnson SC. 2012. A generalized form of context-dependent psychophysiological interactions (gPPI): A comparison to standard approaches. Neuroimage. 61:1277–1286.

Moro V, Pernigo S, Tsakiris M, Avesani R, Edelstyn NMJ, Jenkinson PM, Fotopoulou A. 2016. Motor versus body awareness: Voxel-based lesion analysis in anosognosia for hemiplegia and somatoparaphrenia following right hemisphere stroke. Cortex. 83:62–77.

Nachev P, Kennard C, Husain M. 2008. Functional role of the supplementary and pre-supplementary motor areas. Nat Rev Neurosci. 9:856–869.

Nelissen K, Borra E, Gerbella M, Rozzi S, Luppino G, Vanduffel W, Rizzolatti G, Orban GA. 2011. Action Observation Circuits in the Macaque Monkey Cortex. J Neurosci. 31:3743–3756.

Oldfield RC. 1971. The assessment and analysis of handedness: the Edinburgh inventory. Neuropsychologia. 9:97–113.

Pia L, Spinazzola L, Garbarini F, Bellan G, Piedimonte A, Fossataro C, Livelli A, Burin D, Berti A. 2014. Anosognosia for hemianaesthesia: A voxel-based lesion-symptom mapping study. Cortex. 61:158–166.

Piedimonte A, Garbarini F, Pia L, Mezzanato T, Berti A. 2016. From intention to perception: The case of anosognosia for hemiplegia.

Piedimonte A, Garbarini F, Rabuffetti M, Pia L, Berti A. 2014. Executed and imagined bimanual movements: A study across different ages. Dev Psychol. 50:1073–1080.

Piedimonte A, Garbarini F, Rabuffetti M, Pia L, Montesano A, Ferrarin M, Berti A. 2015. Invisible grasps: Grip interference in anosognosia for hemiplegia. Neuropsychology. 29:776–781.

Porro CA, Francescato MP, Cettolo V, Diamond ME, Baraldi P, Zuiani C, Bazzocchi M, di

Prampero PE. 1996. Primary motor and sensory cortex activation during motor performance and motor imagery: a functional magnetic resonance imaging study. J Neurosci. 16:7688–7698.

Power JD, Barnes KA, Snyder AZ, Schlaggar BL, Petersen SE. 2012. Spurious but systematic correlations in functional connectivity MRI networks arise from subject motion. Neuroimage. 59:2142–2154.

Ramnani N. 2006. The primate cortico-cerebellar system: anatomy and function. Nat Rev Neurosci. 7:511–522.

Rizzolatti G, Fogassi L, Gallese V. 2002. Motor and cognitive functions of the ventral premotor cortex. Curr Opin Neurobiol.

Rizzolatti G, Luppino G. 2001. The Cortical Motor System. Neuron. 31:889–901.

Ronga I, Bazzanella C, Rossi F, Iannetti G. 2012. Linguistic synaesthesia, perceptual synaesthesia, and the interaction between multiple sensory modalities. Pragmat Cogn. 20:135–167.

Rossi S, Hallett M, Rossini PM, Pascual-Leone A. 2009. Safety, ethical considerations, and application guidelines for the use of transcranial magnetic stimulation in clinical practice and research. Clin Neurophysiol. 120:2008–2039.

Rossini P, Burke D, Chen R, Cohen L, Daskalakis Z, Di Iorio R, Di Lazzaro V, Ferreri F, Fitzgerald P, George M, Hallett M, Lefaucheur J, Langguth B, Matsumoto H, Miniussi C, Nitsche M, Pascual-Leone A, Paulus W, Rossi S, Rothwell J, Siebner H, Ugawa Y, Walsh V, Ziemann U. 2015. Non-invasive electrical and magnetic stimulation of the brain, spinal cord, roots and peripheral nerves: Basic principles and procedures for routine clinical and research application. An updated report from an I.F.C.N. Committee. Clin Neurophysiol. 126:1071–1107.

Roth M, Decety J, Raybaudi M, Massarelli R, Delon-Martin C, Segebarth C, Morand S, Gemignani A, Décorps M, Jeannerod M. 1996. Possible involvement of primary motor cortex in mentally simulated movement: a functional magnetic resonance imaging study. Neuroreport. 7:1280–1284.

Sala S Della, Cocchini G, Beschin N, Cameron A. 2009. Vata-m: Visual-Analogue test assessing Anosognosia for motor impairment. Clin Neuropsychol. 23:406–427.

Satterthwaite TD, Elliott MA, Gerraty RT, Ruparel K, Loughead J, Calkins ME, Eickhoff SB, Hakonarson H, Gur RC, Gur RE, Wolf DH. 2013. An improved framework for confound regression and filtering for control of motion artifact in the preprocessing of resting-state functional connectivity data. Neuroimage. 64:240–256.

Smith SM, Nichols TE. 2009. Threshold-free cluster enhancement: Addressing problems of smoothing, threshold dependence and localisation in cluster inference. Neuroimage. 44:83–98.

Stein J. 2009. Cerebellar forward models to control movement. J Physiol. 587:299.

Tanji J, Shima K. 1994. Role for supplementary motor area cells in planning several movements ahead. Nature. 371:413–416.

Vallar G, Ronchi R. 2006. Anosognosia for motor and sensory deficits after unilateral brain damage: a review. Restor Neurol Neurosci. 24:247–257.

Vocat R, Staub F, Stroppini T, Vuilleumier P. 2010. Anosognosia for hemiplegia: A clinical-anatomical prospective study. Brain. 133:3578–3597.

Winkler AM, Ridgway GR, Webster MA, Smith SM, Nichols TE. 2014. Permutation inference for the general linear model. Neuroimage. 92:381–397.

Wittenberg GF, Schaechter JD. 2009. The neural basis of constraint-induced movement therapy. Curr Opin Neurol.

Wolpert DM, Miall RC. 1996. Forward models for physiological motor control. Neural Networks.

Wolpert DM, Miall RC, Kawato M. 1998. Internal models in the cerebellum. Trends Cogn Sci.

Yarkoni T, Poldrack RA, Nichols TE, Van Essen DC, Wager TD. 2011. Large-scale automated synthesis of human functional neuroimaging data. Nat Methods. 8:665–670.

Figures Captions

Figure 1. a) Schematic representation of the study timeline. Orange hands: left manipulated hands (at T1 and T4 left hand is free; at T2 and T3 left hand is blocked with a cast); blue hands: right control hands; fMRI free: motor task with both hands free; fMRI blocked: motor task with the left hand blocked and the right hand free. Between T1 and T2 the left hand was blocked with the cast; between T3 and T4 the cast was removed from left hand. **b)** Experimental task. Visual stimuli presented through RM compatible visual device. Both hands were white in rest condition for 12 seconds. The preparation phase consisted of 12 pictures, presented for 500ms each, of a progressive red painted right hand and a white left hand. When the right hand became whole red and the left hand remained white, participants had to open/close the right hand for 12 seconds. Vice versa for the preparation phase and motor execution of the left hand. In blocked conditions (i.e. T2 and T3), participants were instructed to try to move the left immobilized hand. **c)** ROIs analysis results of execution data: mean beta values ± standard error of M1 activity; Side*Cast interaction. Orange bars: right hemisphere (left hand); blue bars: left hemisphere (right hand). **d)** ROIs analysis results of execution data: mean beta values ± standard error of vPMC activity; Side*Cast interaction. **e)** vPMC bold signal change of execution data normalized on the average of the four time points for each subject: orange and blue dots represent the group average (for right vPMC and left vPMC, respectively), grey dots represent single subject results; Side*Time*Cast interaction. *P < 0.05 Bonferroni corrected. **f)** gPPI results with right vPMC as seed region: Main effect of Cast. The activity of right vPMC was coupled with an increased activity in right S1 (x=+55, y=-17, z=+43).

Figure 2. Anatomo-functional model for motor monitoring during voluntary movement. *Free movements*: When sensory predictions, based on motor programs, match sensory feedbacks of actual movements, the comparator system in PMC is not activated. *Blocked movements*: When sensory predictions, based on motor programs, do not match sensory feedbacks of actual

movements, the comparator in PMC increases its activity and informs the system about the incongruence between motor intention and motor execution.

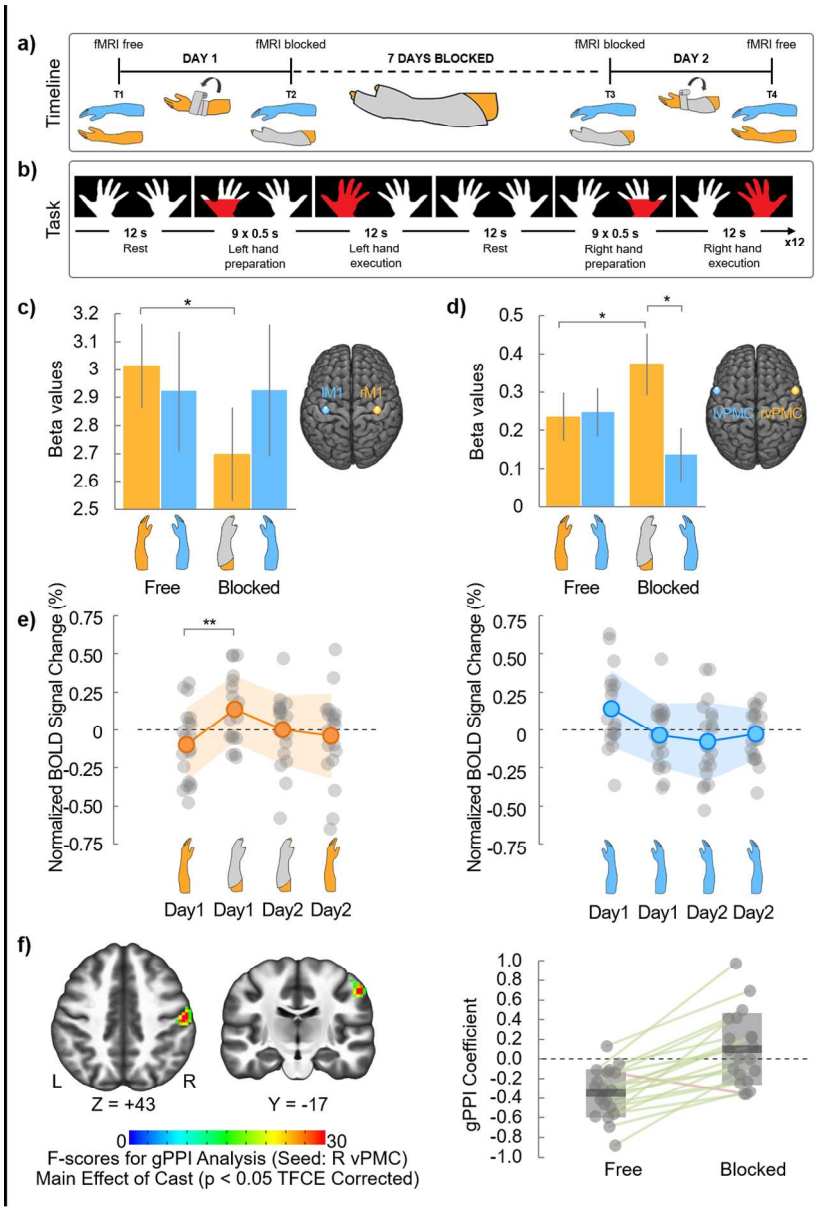

Figure 1. a) Schematic representation of the study timeline. Orange hands: left manipulated hands (at T1 and T4 left hand is free; at T2 and T3 left hand is blocked with a cast); blue hands: right control hands; fMRI free: motor task with both hands free; fMRI blocked: motor task with the left hand blocked and the right hand free. Between T1 and T2 the left hand was blocked with the cast; between T3 and T4 the cast was removed from left hand. b) Experimental task. Visual stimuli presented through RM compatible visual device. Both hands were white in rest condition for 12 seconds. The preparation phase consisted of 12 pictures, presented for 500ms each, of a progressive red painted right hand and a white left hand. When the right hand became whole red and the left hand remained white, participants had to open/close the right hand for 12 seconds. Vice versa for the preparation phase and motor execution of the left hand. In blocked conditions (i.e. T2 and T3), participants were instructed to try to move the left immobilized hand. c) ROIs analysis results of execution data: mean beta values ± standard error of M1 activity; Side*Cast interaction. Orange bars: right hemisphere (left hand); blue bars: left hemisphere (right hand). d) ROIs analysis results of execution data: mean beta values ± standard error of vPMC activity; Side*Cast interaction. e) vPMC

BOLD signal change of execution data normalized on the average of the four time points for each subject: orange and blue dots represent the group average (for right vPMC and left vPMC, respectively), grey dots represent single subject results; Side*Time*Cast interaction. *P < 0.05 Bonferroni corrected. f) gPPI results with right vPMC as seed region: Main effect of Cast. The activity of right vPMC was coupled with an increased activity in right S1 (x=+55, y=-17, z=+43).

110x158mm (300 x 300 DPI)

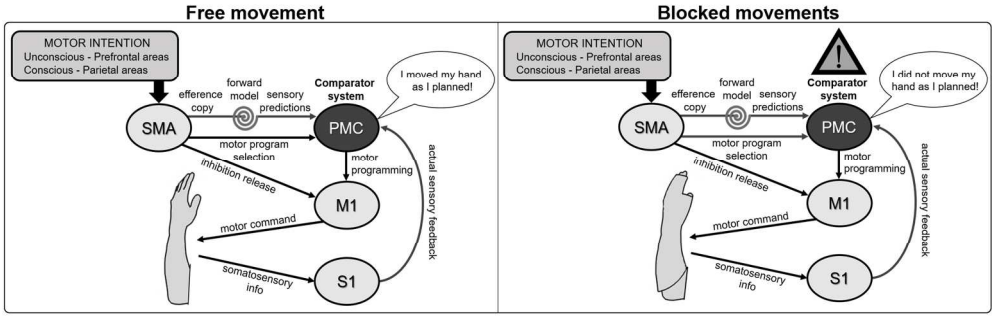

Figure 2. Anatomo-functional model for motor monitoring during voluntary movement. Free movements: When sensory predictions, based on motor programs, match sensory feedbacks of actual movements, the comparator system in PMC is not activated. Blocked movements: When sensory predictions, based on motor programs, do not match sensory feedbacks of actual movements, the comparator in PMC increases its activity and informs the system about the incongruence between motor intention and motor execution.

169x56mm (300 x 300 DPI)

Additional whole-brain analysis

Methods

Voxelwise whole-brain analyses were used to assess differences between T1 and all the other time-points, to corroborate the results derived from the ROI-based approach. In this regard, β-values maps obtained from single-subjects GLM analysis (please refer to the main manuscript for further details) served as inputs for two separate paired T-tests (T1 vs T2 and T1 vs T3), so as to assess the influence of immobilization on brain activity evoked by left hand motor execution task. For the sake of completeness, we also tested differences in brain activity between the first (namely baseline activity) and the fourth time-point. Statistical significance of each resulting map has been established using a robust non-parametric permutation approach (FSL randomize; Jenkinson et al., 2012) and the threshold-free cluster enhancement method (TFCE; Smith and Nichols, 2009).

Results

The results for these supplementary analyses showed that the activity of the right ventral portion of the precentral sulcus (R PreCS) is significantly higher immediately after immobilization of the left hand (i.e., T2 > T1; Supplementary Figure 2), while is not different from baseline (i.e., T1) after one week of movement restriction (i.e., T3). In addition, location of the R PreCS cluster (54, 14, 29) closely resembles the coordinates of right vPMC independently established using Neurosynth (56, 6, 30). Two additional clusters emerged from the whole-brain analysis when comparing brain activity at baseline (i.e., T1) and immediately after immobilization (i.e., T2): the left supramarginal gyrus and the right postcentral sulcus. Lastly, the comparison of brain activity across timepoints (i.e., T1 vs T2; T1 vs T3; T1 vs T4) did not reveal any other significant difference.

References

Jenkinson, M., Beckmann, C. F., Behrens, T. E., Woolrich, M. W., & Smith, S. M. (2012). Fsl. Neuroimage, 62(2), 782-790.

Smith, S. M., & Nichols, T. E. (2009). Threshold-free cluster enhancement: addressing problems of smoothing, threshold dependence and localisation in cluster inference. Neuroimage, 44(1), 83-98.

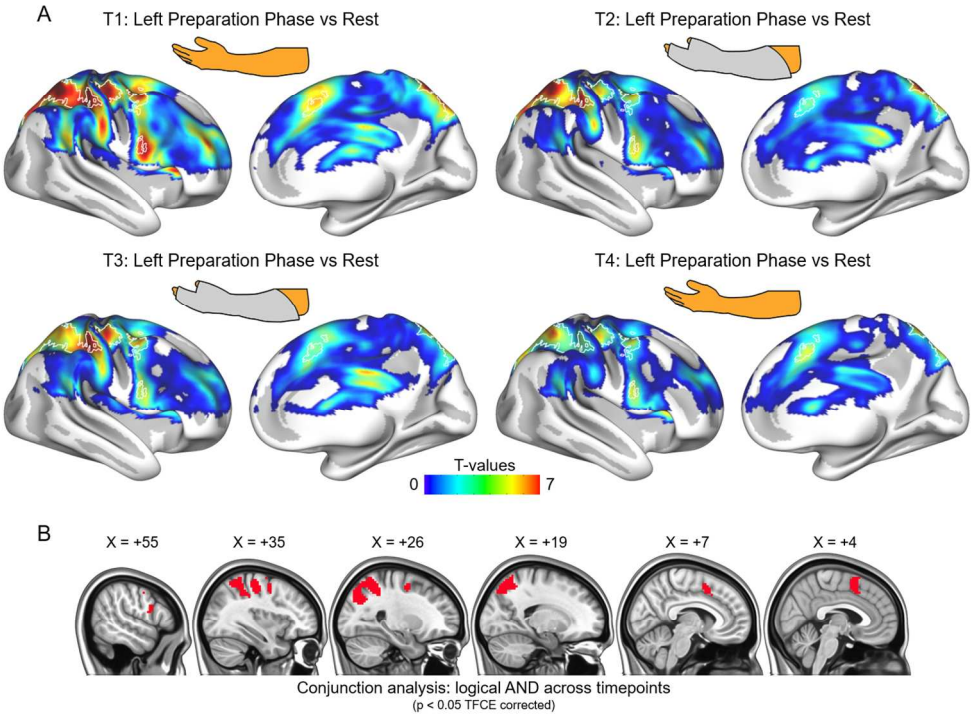

Supplementary Figure 1. This figure depicts brain activity elicited by the preparation phase for the left hand movement at different timepoints (A). For each timepoint, a whole-brain voxelwise analysis identifies brain regions engaged during preparation phase: unthresholded statistical maps (T-values) are reported and the white outline represents clusters found to be significantly recruited ($p < 0.05$ TFCE corrected) in all the four timepoints (logical 'AND' mask). Panel C shows voxels significantly recruited in all the four timepoints: other than primary and supplementary motor and dorsal and ventral premotor cortices, preparation phase determines an increase of hemodynamic activity in the superior parietal lobule, as compared to the motor execution phase.

129x95mm (300 x 300 DPI)

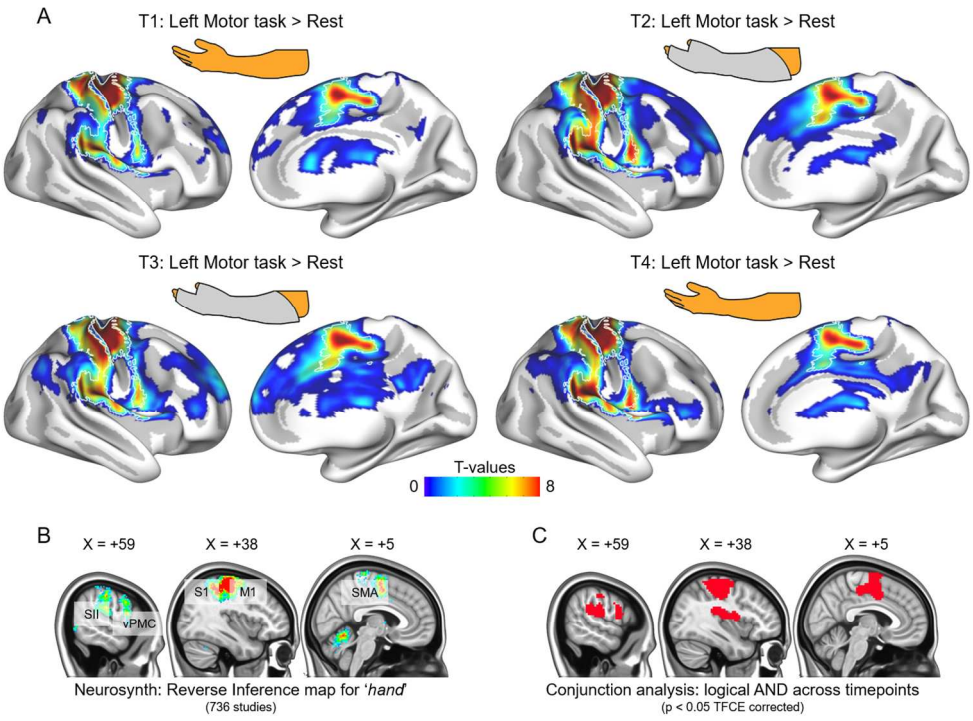

Supplementary Figure 2. Panel A shows the results of motor execution task for the left hand at different timepoints. For each timepoint, a whole-brain voxelwise analysis identifies brain regions engaged during motor execution: unthresholded statistical maps (T-values) are reported and the white outline represents clusters found to be significantly recruited ($p < 0.05$ TFCE corrected) in all the four timepoints (logical 'AND' mask). Panel B shows the reverse inference meta-analytic map for the term 'hand' as computed by pooling together 736 fMRI studies in Neurosynth. The obtained map provides an accurate and comprehensive description of the somato-motor hand network, entailing primary (S1) and secondary (SII) somatosensory cortices, primary (M1) and supplementary (SMA) motor areas, and dorsal (not shown) and ventral premotor (vPMC) cortices, among other regions. Moreover, this map closely resembles the one obtained by selecting voxels significantly engaged by motor execution in all the four timepoints (C). Please note that the network derived from our data does not include the cerebellum, due to partial coverage acquisition.

129x95mm (300 x 300 DPI)

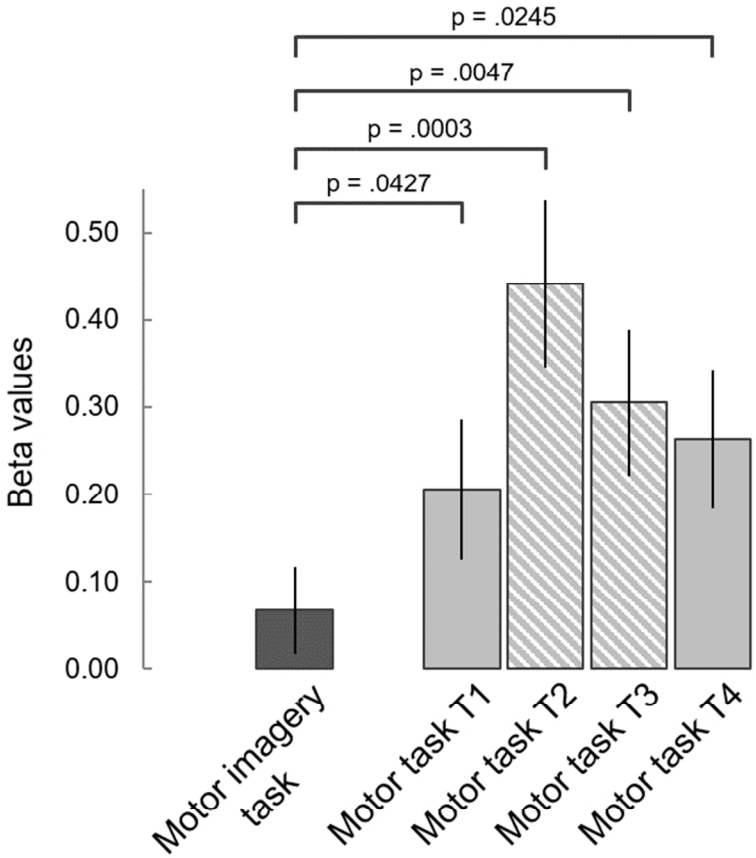

Supplementary Figure 3. The figure shows average activity ± standard error of the right vPMC during mental imagery (dark grey column; "Imag") and actual execution (light grey columns; "Exec T1", "Exec T4") of left hand movement and activity of the same region during the attempt to move the immobilized left hand (dashed columns; "Exec T2", "Exec T3"). Activity of the right vPMC is significantly higher for all the four timepoints (i.e., T1 to T4) as compared to mental imagery.

69x66mm (300 x 300 DPI)

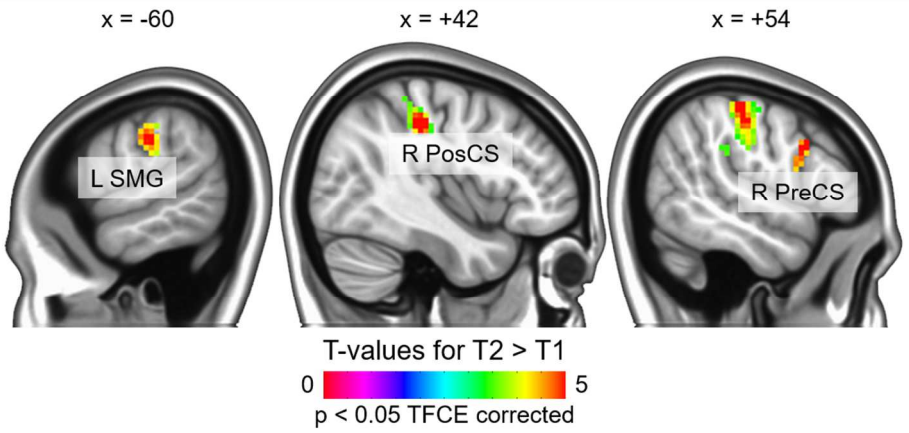

Brain Region	X	Y	Z	Cluster Size	T-value
Right Postcentral Sulcus	42	-28	41	8316 mm^3	6.39
Left Supramarginal Gyrus	-60	-22	35	3618 mm^3	5.35
Right Precentral Sulcus	54	14	29	513 mm^3	5.31

Supplementary Figure 4. Here, results for the whole-brain voxelwise contrast between T2 (Day 1, Cast) versus T1 (Day 1 Free) are shown. The right inferior bank of the precentral sulcus (R PreCS) was more recruited immediately after immobilization (i.e., T2), when subjects attempt to move the immobilized (left) hand, as compared to the unrestrained condition (i.e., T1). Peak location for this difference well matched the coordinates for vPMC, obtained using Neurosynth meta-analytic approach. Other regions differentially engaged in these two timepoints were the right postcentral sulcus (R PosCS), and the anterior portion of the left supramarginal gyrus (L SMG).

103x72mm (300 x 300 DPI)

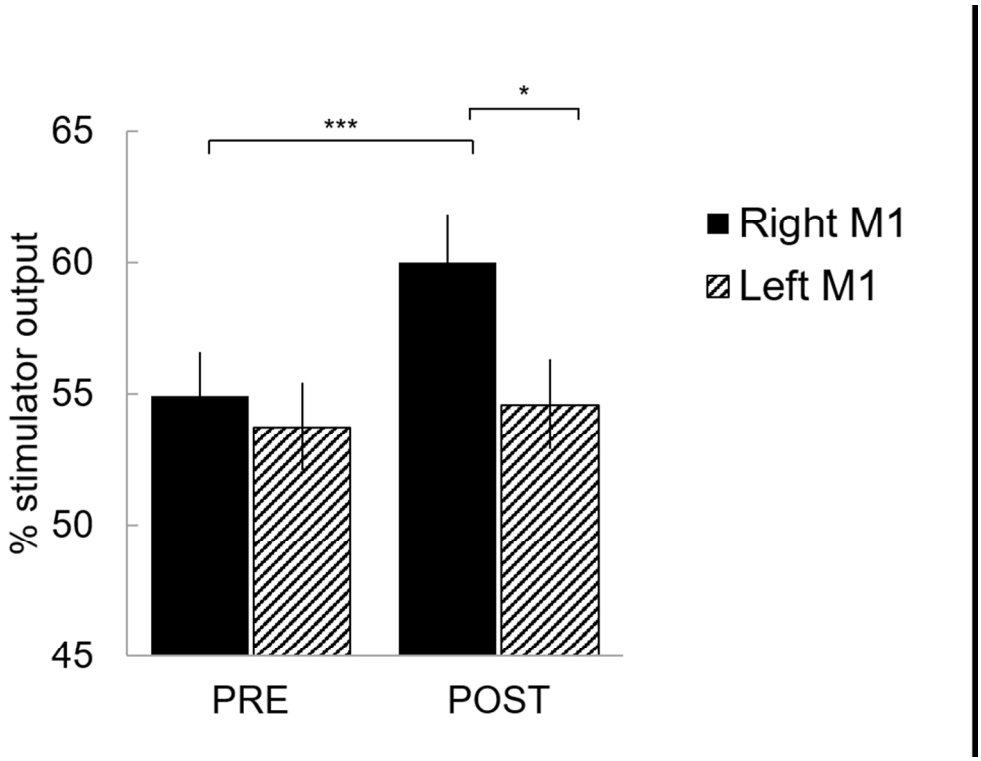

Supplementary Figure 5. Mean values of rMT ± standard error, expressed as percentage of the stimulator output. PRE: one week prior to T1; POST: immediately after T4. *P < 0.05, ***P < 0.001.

83x62mm (300 x 300 DPI)

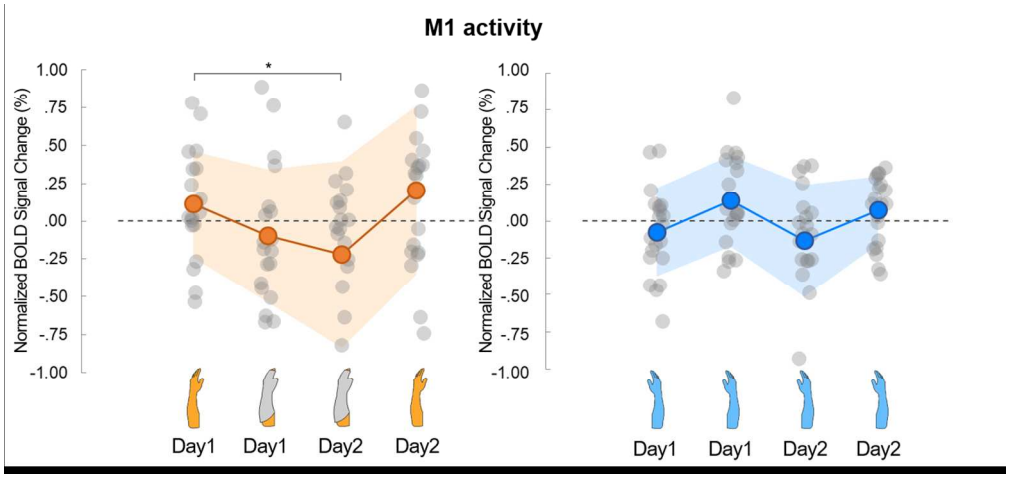

Supplementary Figure 6. M1 BOLD signal change of execution data normalized on the average of the four time points for each subject: orange and blue dots represent the group average (for right M1 and left M1, respectively), grey dots represent single subject results; *P < 0.05 paired T-test (two-tailed). Please note the progressive reduction of the BOLD signal in blocked conditions through time. The only significant difference is between the baseline free condition at Day 1 (T1) and the blocked condition of Day 2 (T3).

121x57mm (300 x 300 DPI)